

A genome-wide association study with tissue transcriptomics identifies genetic drivers for classic bladder exstrophy

Enrico Mingardo^{1,2,3,59}, Glenda Beaman^{4,59}, Philip Grote^{5,6,59}, Agneta Nordenskjöld^{7,8}, William Newman⁴, Adrian S. Woolf^{9,10}, Markus Eckstein^{11,12,13}, Alina C. Hilger^{3,14}, Gabriel C. Dworschak^{1,3}, Wolfgang Rösch¹⁵, Anne-Karolin Ebert¹⁶, Raimund Stein¹⁷, Alfredo Brusco¹⁸, Massimo Di Grazia¹⁹, Ali Tamer⁵, Federico M. Torres²⁰, Jose L. Hernandez²¹, Philipp Erben^{13,22}, Carlo Maj²³, Jose M. Olmos²⁴, Jose A. Riancho²⁴, Carmen Valero²⁴, Isabel C. Hostettler^{25,26,27}, Henry Houlden²⁸, David J. Werring²⁹, Johannes Schumacher³⁰, Jan Gehlen³⁰, Ann-Sophie Giel³⁰, Benedikt C. Buerfent³⁰, Samara Arkani^{31,32}, Elisabeth Åkesson^{33,34}, Emilia Rotstein³⁵, Michael Ludwig³⁶, Gundela Holmdahl³⁷, Elisa Giorgio^{38,39}, Alfredo Berettini⁴⁰, David Keene⁴¹, Raimondo M. Cervellione⁴¹, Nina Younsi¹⁷, Melissa Ortlieb¹⁶, Josef Oswald⁴², Bernhard Haid^{17,42}, Martin Promm¹⁵, Claudia Neissner¹⁵, Karin Hirsch⁴³, Maximilian Stehr⁴⁴, Frank-Mattias Schäfer^{44,45}, Eberhard Schmiedeke⁴⁶, Thomas M. Boemers⁴⁷, Iris A. L. M. van Rooij⁴⁸, Wouter F. J. Feitz⁴⁹, Carlo L. M. Marcelis⁵⁰, Martin Lacher⁵¹, Jana Nelson⁵¹, Benno Ure⁵², Caroline Fortmann⁵², Daniel P. Gale⁵³, Melanie M. Y. Chan⁵³, Kerstin U. Ludwig³, Markus M. Nöthen³, Stefanie Heilmann^{3,54}, Nadine Zwink⁵⁵, Ekkehart Jenetzky^{55,56}, Benjamin Odermatt^{1,2}, Michael Knapp^{57,59} & Heiko Reutter^{3,58,59}

Classic bladder exstrophy represents the most severe end of all human congenital anomalies of the kidney and urinary tract and is associated with bladder cancer susceptibility. Previous genetic studies identified one locus to be involved in classic bladder exstrophy, but were limited to a restrict number of cohort. Here we show the largest classic bladder exstrophy genome-wide association analysis to date where we identify eight genome-wide significant loci, seven of which are novel. In these regions reside ten coding and four non-coding genes. Among the coding genes is EFNA1, strongly expressed in mouse embryonic genital tubercle, urethra, and primitive bladder. Re-sequencing of EFNA1 in the investigated classic bladder exstrophy cohort of our study displays an enrichment of rare protein altering variants. We show that all coding genes are expressed and/or significantly regulated in both mouse and human embryonic developmental bladder stages. Furthermore, nine of the coding genes residing in the regions of genome-wide significance are differentially expressed in bladder cancers. Our data suggest genetic drivers for classic bladder exstrophy, as well as a possible role for these drivers to relevant bladder cancer susceptibility.

The bladder exstrophy-epispadias complex (BEEC) is a spectrum of congenital abnormalities which involves the abdominal wall, bony pelvis, the urinary tract, the external genitalia, and in the worse cases also the gastrointestinal tract. The BEEC represents the severe end of all human congenital anomalies of the kidney and urinary tract. The most common defect form, classic bladder exstrophy (CBE), is characterized by pubic diastasis, the evaginated bladder plate template, and an epispadic urethra. At birth, the visible bladder mucosa appears reddish and mucosal polyps may be seen on the surface. CBE is associated with kidney and other upper urinary tract anomalies with a higher occurrence in males compared to females¹. Associated long-term complications include malignancies of the bladder comprising mainly urothelial cell carcinoma and adenocarcinoma^{2,3}. Recently, the CBE live prevalence for Germany has been estimated to be ~1:30,700⁴. Given the overall European population of ~450,000,000 (<https://ec.europa.eu/>) citizens, presumptively ~15,000 CBE patients live in Europe. State-of-the-art health care for this population should take the genetic and bladder cancer disposition into account.

To determine the genetic contribution to CBE, we previously performed two genome-wide association studies (GWAS) with subsequent meta-analysis and identified a susceptibility locus on chromosome 5q11.1^{5,6}. The present study aimed to identify further risk loci. Furthermore, we investigated if the identified genetic risk loci might be involved in the associated bladder cancer susceptibility. For this purpose, we performed the largest GWAS for CBE to date comprising 628 patients and 7352 ethnically matched controls. In detail, the present meta-analysis included seven independent discovery samples (Supplementary Information: Supplementary Table 1) comprising: 98 patients of Central European origin and 526 ethnically matched controls⁵, 110 patients of Central European origin and 1,177 ethnically matched controls⁶, 172 patients of Central European origin and 2588 ethnically matched controls, 57 patients of Italian origin and 1,325 ethnically matched controls, 62 patients of Spanish origin and 279 ethnically matched controls, 80 patients of Swedish origin and 238 ethnically matched controls, and 49 patients of UK origin and 1,219 ethnically matched controls, identifying eight genome-wide significant risk loci, seven of which are novel. Within these loci reside 10 coding genes (*LPHN2*, *EFNA1*, *SLC50A1*, *DPM3*, *KRTCAP2*, *ISL1*, *TRIM29*, *SYT1*, *PAWR*, *GOSR2*) and four non-coding genes (one pseudogene and three long non-coding RNA, respectively, *HMGB1P47*, *ISL1-DT*, *LINC01974*, and *LINC01716*). Among these coding genes, *EFNA1* has been previously shown to be strongly expressed in mouse embryonic genital tubercle, urethra, and primitive bladder prompting us to re-sequence this gene in our cohort. To assess their embryonic and fetal expression, we generated mouse embryonic bladder total RNA-seq at CBE-relevant developmental stages E10.5, E12.5, and E15.5, and human embryonic and fetal urinary bladder and genital tissues total RNA-seq at gestational week 7, 7 to 7.5, 7.5, 8, and 9. Finally, to evaluate their possible link in the overall CBE bladder cancer susceptibility, we analyzed the expression of these genes in urothelial carcinoma tissues and in different bladder cancer cell lines obtained from the Cancer Cell Line Encyclopedia (EMBL-EBI) compared to healthy bladder tissue transcriptomic (GEO).

Results

GWAS meta-analysis. The meta-analysis of 628 patients with CBE and 7,352 ethnically matched controls comprised seven independent GWAS. These seven GWAS included the first two GWAS cohorts^{5,6}, and five new CBE cohorts described above from Central European, Italy, Spain, Sweden, and the UK along

with ethnically matched control samples. We used a total of 8,289,003 SNPs with info score >0.4 and mean dosage for the minor allele >1% in cases and controls in at least one sample, obtaining a genomic inflation factor λ of 1.068. The respective Q-Q plot is shown in Supplementary information (Supplementary Fig. 16). Single marker analysis identified eight genome-wide significant loci shown in the Manhattan plot in Supplementary information (Supplementary Fig. 17) and the strongest signal at rs6874700 $p = 5.58 \times 10^{-24}$ corresponds to the 5q11.1 previously reported locus (Fig. 1)⁶. Table 1 shows the relative risks in each sample and in the meta-analysis for the most strongly associated SNP (top SNP) from each locus. Notably, with the exception of the UK sample where the top associated SNP on chromosome 12 was not significant, the direction of effect was consistent between all studies for these top SNPs. A complete list of all genome-wide significant SNPs is given in Supplementary Data 2. Regional association results for all eight genome-wide significant loci are shown in Fig. 1 and in Supplementary Information (Supplementary Figs. 1–8). For conditional logistic regression analyses the regional association plots are presented in Supplementary Information (Supplementary Figs. 20–27). The results provide no evidence that secondary signals in any of the eight loci are present.

Re-sequencing of *EFNA1*. Among the most significant markers, marker rs4745 resides directly in *EFNA1*. Mouse *Efna1* has been shown to be expressed in CBE-relevant embryonic anatomical structures (<https://www.gudmap.org/>). This prompted us to re-sequence *EFNA1* in 580 CBE patients. We identified 14 rare variants in 14 independent patients (Supplementary information, Supplementary Table 4). Four of these variants residing in the coding region of *EFNA1* were found to be novel: two heterozygous missense variants c.116 T > C (p.Ile39Thr) and c.503 C > T (p.Alal68Val); one homozygous missense variant c.167 A > G (p.Asp56Gly), and a heterozygous loss of function (LoF) frameshift variant at c.341delT (p.Phe114Serfs*28). Parental samples were only available for the patient carrying variant c.116 T > C demonstrating paternal transmission. In silico prediction tools, Mutation Taster, Poly-Phen-2, and SIFT defined the missense variant c.116 T > C (p.Ile39Thr) as disease-causing, deleterious, and possibly damaging. The CADD score of 25.3 supports a functional implication of this variant on *EFNA1* regulation. None of the other missense variants were scored deleterious. The LoF variant c.341delT (p.Phe114Serfs*28) has a CADD score of 25.6. For the estimation of the enrichment of rare protein-altering variants in *EFNA1* in our cohort compared to the general population resembled by gnomAD, we use a very conservative comparison. Hence, we only included the three novel coding variants with CADD score >20, identified here in our re-sequencing approach of *EFNA1*. We compared these to missense or LoF variants in gnomAD less or equal to 5 (≤ 5 in 250,000; MAF ≤ 0.00002) consistent with rare penetrant dominant phenotypes. These criteria identified 162 missense and LoF variants in gnomAD (baseline 250,000 alleles; https://gnomad.broadinstitute.org/gene/ENSG00000169242?dataset=gnomad_r2_1). Per se, it is possible that some of these variants are cis/trans in the same individuals but if we would be able to define this it would only make the association stronger. For comparison, we used Fisher's exact test. Taking this assumption, the chi-square statistic using Fisher's exact test, yielded 18.0159, and the p value is 0.000022. We added this statistic to our results.

Analysis of mouse and human embryonic total RNA-sequencing data of the identified genes in mouse and human embryonic and fetal urinary bladder and genital tissues. In the linkage disequilibrium block of all eight top SNPs reside 10

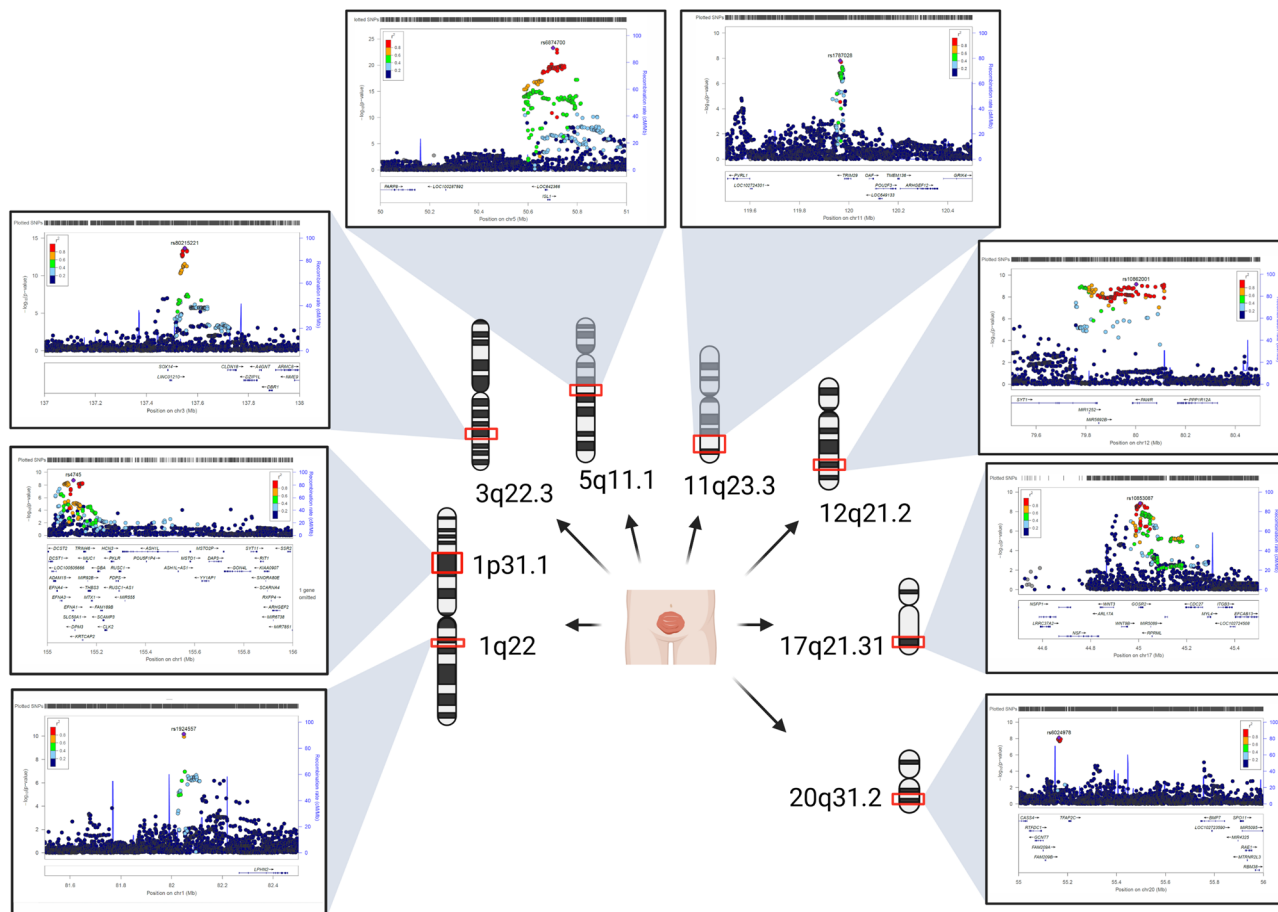


Fig. 1 Chromosome regional association loci of CBE. The eight CBE regional association loci (red boxes in chromosomes) reside in chromosome 1, 3, 5, 11, 12, 17, and 20. In the panels, details of the genome-wide association loci: every dot represents an SNP (x axes) plotted to the relative $-\log_{10}(P)$ value (y axes). SNP are colored according to the relative r^2 value.

coding genes, four non-coding genes comprising one pseudogene, and three Long Intergenic Non-Protein Coding RNAs (Table 2). All 10 coding genes showed expression in mouse embryonic bladder at E10.5, E12.5, and E15.5. *Isl1*, *Trim29*, *Syt1*, and *Pawr* showed differential expression through different mouse embryonic stages (Table 3, Fig. 2a). As in mouse transcriptome, all 10 coding genes showed expression in the human embryonic bladder during different developmental stages. *DPM3*, *TRIM29*, *SYT1*, and *PAWR* showed differential expression at different human embryonic respectively fetal stages (Table 3, Fig. 2b). While the two *LINC01974* and *LINC01716* are not expressed in any of the bladder developmental stages, the pseudogene *HMGB1P45* and the long noncoding RNA *ISL1-DT* are strongly downregulated; the first from weeks 7 to 7.5 followed by gene silencing at week 8 and 9 and the latter shows a downregulation trend from weeks 7 to 9.

Comparison of RNA-sequencing data of the identified genes in healthy bladder tissue and different types of bladder cancer cell lines and muscular invasive urothelial carcinoma. Expression of non-coding genes in healthy bladder tissue and muscular invasive urothelial carcinoma could not be detected due to polyA-RNA-sequencing (Table 4). Despite this, we found all coding genes to be differentially expressed when compared to healthy bladder tissue (Table 5, Fig. 2c). In detail, *SLC50A1* and *SYT1* were significantly upregulated in all cancers compared to healthy bladder tissue. On contrary, *DPM3* and *KRTCAP2* were significantly downregulated. All other coding genes *LPHN2*, *EFNA1*, *ISL1*,

TRIM29, *PAWR*, and *GOSR2* were differentially up- or down-regulated in different cancers (Table 5, Fig. 2c).

Discussion

Recently, we described *SLC20A1*, encoding a sodium-phosphate symporter, as the putative monogenic dominant disease gene for isolated BEEC⁷. We were able to support our genetic data through functional studies in non-BEEC human embryos, mouse embryos, and zebrafish Morpholino knockdown experiments. To our knowledge, the present genetic study with a focus on the multifactorial genetic background of the BEEC is the largest study on CBE to date. We identified eight genome-wide significant risk loci. Within these loci, we determined possible CBE candidate genes using transcriptome datasets of CBE-relevant mouse embryonic, human embryonic, and fetal urogenital tissues at different developmental stages. Additionally, we provide a possible link between the identified putative candidate genes and CBE-associated bladder cancer susceptibility.

In detail, in direct proximity to the most significant markers of all eight risk loci reside nine coding genes that are expressed in CBE-relevant mouse and human urogenital tissues during different embryonic stages. Four of these candidate genes (*Isl1*, *Trim29*, *Syt1*, *Pawr*) showed differential expression in mouse embryonic urogenital tissues, five of these candidate genes (*DPM3*, *ISL1*, *TRIM29*, *SYT1*, and *PAWR*), and two of the non-coding genes (*HMGB1P47*, *ISL1-DT*) showed differential expression in human embryonic urogenital tissues. Previous reports of transgenic mouse lines of *Isl1* and *Syt1* revealed

Table 1 Top SNPs from genome-wide significant loci.

SNP	Chromosome	risk/ other allele	Info Score ¹	GWAS1		GWAS2		CE		Italy		Spain		Sweden		UK		Meta-analysis		Corrected p value ²
				RR	(95% CI)	RR	(95% CI)	RR	(95% CI)	RR	(95% CI)	RR	(95% CI)	RR	(95% CI)	RR	(95% CI)	RR	(95% CI)	
rs1924557	1:82047934	T/C	0.93	1.75 (0.68–4.47)	3.61 (1.37–9.49)	3.76 (2.16–6.53)	2.03 (0.98–4.19)	3.51 (1.33–9.26)	1.23 (0.68–2.22)	5.00 (1.59–15.7)	2.35 (1.82–3.03)	6.65 × 10 ⁻¹¹	2.67 × 10 ⁻¹⁰							
rs4745	1:155106227	T/A	0.96	1.19 (0.72–1.98)	1.40 (0.91–2.16)	1.47 (1.16–1.87)	1.80 (1.16–2.78)	1.17 (0.73–1.86)	1.63 (1.13–2.36)	1.16 (0.77–1.74)	1.50 (1.32–1.71)	4.44 × 10 ⁻¹⁰	1.58 × 10 ⁻⁹							
rs80215221	3:137550420	G/A	0.99	2.29 (1.29–4.09)	1.95 (1.20–3.17)	1.39 (1.08–1.79)	1.89 (1.24–2.89)	2.82 (1.76–4.52)	1.70 (1.16–2.51)	1.99 (1.31–3.03)	1.68 (1.47–1.92)	2.26 × 10 ⁻¹⁴	1.49 × 10 ⁻¹³							
rs6874700	5:50701750	A/T	0.99	2.54 (1.49–4.33)	1.33 (0.87–2.02)	1.60 (1.28–2.01)	1.98 (1.33–2.95)	2.14 (1.33–3.45)	1.94 (1.32–2.83)	1.84 (1.20–2.80)	1.91 (1.68–2.16)	5.58 × 10 ⁻²⁴	1.48 × 10 ⁻²²							
11:119964758;G:C	11:119964758	G/C	0.98	1.38 (0.81–2.36)	1.54 (0.98–2.42)	1.32 (1.03–1.69)	1.35 (0.90–2.04)	1.14 (0.72–1.80)	1.68 (1.12–2.52)	2.13 (1.40–3.24)	1.47 (1.29–1.68)	8.89 × 10 ⁻⁹	2.63 × 10 ⁻⁸							
rs10862001	12:80002106	A/G	0.83	2.02 (1.12–3.64)	1.48 (0.89–2.47)	1.77 (1.27–2.45)	1.97 (1.22–3.18)	1.03 (0.55–1.93)	2.11 (1.26–3.54)	0.83 (0.40–1.69)	1.68 (1.43–1.99)	6.84 × 10 ⁻¹⁰	2.37 × 10 ⁻⁹							
rs10853087	17:45006112	C/G	0.97	1.18 (0.72–1.93)	1.44 (0.94–2.21)	1.63 (1.29–2.06)	1.60 (1.08–2.38)	1.46 (0.93–2.29)	1.26 (0.87–1.83)	1.53 (1.01–2.31)	1.47 (1.30–1.66)	1.41 × 10 ⁻⁹	4.67 × 10 ⁻⁹							
20:55165923;G:A	20:55165923	G/A	0.97	2.30 (1.13–4.67)	1.72 (0.95–3.12)	1.46 (1.08–1.98)	2.57 (1.39–4.76)	1.00 (0.58–1.71)	2.08 (1.23–3.51)	1.89 (1.04–3.43)	1.65 (1.39–1.96)	7.31 × 10 ⁻⁹	2.19 × 10 ⁻⁸							

¹Mean imputation quality score (info score). Chromosomal positions are annotated according to Human Genome version 19 (hg19); CE Central Europe, UK United Kingdom
²p value corrected for genomic inflation λ = 1.068

phenotypic overlap to the human CBE phenotypic spectrum. The *Hoxb6Cre;Isl1* cKO hindlimb skeletons exhibited proximal defects in particular the os pubis and ischium, two posterior segments of the pelvic girdle, were missing, resembling pubic diastasis, a human BEEC-specific feature^{1,8}. Transgenic *Syt1^{tm1a}(EUCCOMM)^{Wtsi}/Syt1^{tm1a}(EUCCOMM)^{Wtsi}* mice among other features develop thoracoschisis⁹, a rare congenital anomaly characterized by the evisceration of intra-abdominal organs through a thoracic wall defect¹⁰ mirroring the BEEC associated infraumbilical abdominal wall defect¹.

One of the most significant markers identified in the present GWAS resides within *EFNA1*. In general, a probability of being LoF intolerant (pLi) score of 0.46 for *EFNA1* is suggestive of possessing LoF intolerance for this gene in the context of the CBE condition. Although the pLi of 0.46 is only suggestive of LoF we have to consider that bladder exstrophy is not a mortal condition at birth. Hence, we believe that a value of 0.46 is supportive for *EFNA1* to be implied in CBE¹¹. Previously, in *EFNA1* only two LoF variants were observed in the entire gnomad (frequency of 0,000016). Here, we observed one in 580 (frequency of 0,0017). Furthermore, in *EFNA1* in the entire gnomad database, 96 missense variants were observed in 125,099 individuals (frequency of 0,00077). Here, we identified three in 580 (0,0052). Based on this observation, we performed a conservative estimation of whether LoF or missense variants might be enriched in *EFNA1* in our CBE cohort compared to the general population showing a significant difference between both cohorts (*p* 0.000022). This finding suggests a possible implication of these variants in CBE formation in a multifactorial inheritance model among the affected.

Comparative analysis of control and bladder cancer tissues showed that all of the ten candidate genes were differentially expressed in bladder cancers. *SLC50A1* and *SYT1* were significantly upregulated in all cancers compared to healthy bladder tissue. On contrary, *DPM3* and *KRTCAP2* were significantly downregulated. *LPHN2* has been suggested to have a regulatory role in urothelial bladder cancer¹². *EFNA1* plays a pivotal role in the pathogenesis of several tumors, including renal cell carcinoma, bladder, and prostate cancer^{13,14}. Mapping all putative candidate genes prioritized in the present study to the search tool for retrieval of interacting genes (STRING), we found probable interaction of three proteins comprising: (i) gene fusions between *EFNA1* and *SLC50A1*, and (ii) co-expression between *EFNA1* and *DPM3*, (iii) and *EFNA1* and *SLC50A1* (Supplementary information: Supplementary Fig. 28). The PPI enrichment p-value was determined with 0.000205. Gene clustering analysis suggested clustering for *EFNA1*, *DPM3*, and *SLC50A1* (Supplementary information: Supplementary Fig. 28). All three genes *EFNA1*, *DPM3*, and *SLC50A1*, respectively the genomic region 1q21-q22, been previously associated with the 2D:4D ratio, a sexually dimorphic trait, that has been extensively used in adults as a biomarker for prenatal androgen exposure¹⁵. Markers in the region of *EFNA1*, *DPM3*, *SLC50A1* have previously been associated with prostate cancer risk¹⁶. Prostate cancer risk on the other side correlates with serum testosterone levels¹⁷. All of these observations suggest a possible gene-environmental interaction for this region. Adding to this hypothesis in the context of embryonic CBE formation, CBE presents with a higher occurrence rate in males compared to females¹, a skewed sex ratio that is so far not explained, but could be influenced by differences in intrauterine androgen exposure between males and females.

The tumor suppressor gene *TRIM29* is up regulated during early and late embryonic bladder development but is down-regulated in three different bladder cancers¹⁸. More specific, *TRIM29* protein has been shown to be a driver of invasive and non-invasive bladder cancer. Interestingly, *TRIM29*-driven bladder cancers in transgenic mice were indistinguishable from

Table 2 Coding and non-coding genes in the LD blocks of the most significant markers for CBE.

Gene name	Associated SNP	Protein encoded	Type	Cellular location	Function
LPHN2	rs1924557	Adhesion G protein-coupled receptor L2	G protein-coupled receptor	Transmembrane of plasma membrane	Exocytosis regulator
EFNA1	rs4745	Ephrin-A1	Tyrosine kinase receptor	Transmembrane of plasma membrane	GPI-bound ligand for Eph receptors, involved in cell migration, repulsion, and adhesion
SLC50A1	rs4745	Solute Carrier Family 50 Member 1	Glucose transporter	Transmembrane of plasma membrane	Sugar transport across membranes
DPM3	rs4745	Dolichol-phosphate mannosyltransferase subunit 3	Synthase of mannosyl residual	Endoplasmic reticulum membrane	Stabilizer subunit of DPM complex (DPM1, DPM2, and DPM3)
KRTCAP2	rs4745	Keratinocyte-associated protein 2	Subunit of the oligosaccharyl transferase complex	Endoplasmic reticulum membrane	Protein N-glycosylation. Transfer of defined glycan (Glc(3)Man(9)GlcNAc(2). DNA-binding transcriptional activator
ISL1	rs6874700	Insulin Gene Enhancer Protein ISL-1	Transcription Factor	Nucleus	
TRIM29	11:119964758	Tripartite motif-containing protein 29	Zinc finger and Leucine zipper motif		Nucleic acid binding and macrophage activation
SYT1	rs10862001	Synaptotagmin-1	Ca(2+) sensor		Triggering neurotransmitter release
PAWR	rs10862001	Pro-Apoptotic WTI Regulator	Apoptosis inducer	Transmembrane of synaptic vesicles	Downregulation of BCL2 via its interaction with WTI
GOSR2	rs10853087	Golgi SNAP receptor complex member 2	Trafficking membrane protein	Nucleus and cytoplasm Golgi	Protein transport from the cis-medial-Golgi
LINC01974	rs10853087	/	Long ncRNA	Unknown	Unknown
LINC01716	20:55165923	/	Long ncRNA	Unknown	Unknown
HMGBlP47	rs6874700	/	Long ncRNA	Unknown	Unknown
ISL1-DT	rs6874700	/	Long ncRNA. ISL1 divergent transcript.	Unknown	Unknown

Table 3 RNA expression patterns of coding and non-coding genes in the LD blocks of the most significant GWAS markers in mouse and human embryonic urogenital tissue.

Mouse embryonic transcriptome data					Human embryonic transcriptome data						
Marker	Gene	log2fc E10.5 vs. E12.5	log2fc E10.5 vs. 15.5	log2fc E12.5 vs. 15.5	Gene	log2fc 7 vs. 7-7.5	log2fc 7-7.5 vs. 7.5	log2fc 7 vs. 7.5	log2fc 7.5 vs. 8	log2fc 7 vs. 9	log2fc 8 vs. 9
rs1924557	LPHN2	-0.21	0.57	-1.16	LPHN2	0.16	-0.54	-0.38	0.09	-0.10	0.19
rs4745	EFNA1	-0.12	-0.76	-0.64	EFNA1	-0.25	-0.34	-0.58	0.00	-0.30	0.28
rs4745	SLC50A1	0.80	1.34	0.54	SLC50A1	0.03	0.07	0.10	-0.28	-0.18	0.00
rs4745	DPM3	0.06	0.86	0.81	DPM3	0.00	-1.72	-1.72	0.19	-0.52	1.00
rs4745	KRTCAP2	0.27	0.31	-0.04	KRTCAP2	-0.58	0.00	-0.58	0.58	-0.58	0.58
rs6874700	ISL1	-0.26	-5.01	-4.76	ISL1	-1.26	0.88	-0.38	-1.37	-1.48	0.28
11:119964758	TRIM29	1.90	1.10	-0.80	TRIM29	2.00	-1.26	0.74	0.00	1.87	1.14
rs10862001	SYT1	2.85	2.41	-0.44	SYT1	-0.25	1.04	0.79	-2.54	0.08	1.8
rs10862001	PAWR	-0.32	1.37	1.69	PAWR	0.70	0.55	1.25	-1.66	0.32	0.74
rs10853087	GOSR2	-0.16	-0.44	-0.28	GOSR2	-0.14	0.34	0.19	-0.19	-0.14	-0.14

Marker	Non-coding Gene	log2fc E10.5 vs. E12.5	log2fc E10.5 vs. 15.5	log2fc E12.5 vs. 15.5	Non-coding gene	log2fc 7 vs. 7-7.5	log2fc 7-7.5 vs. 7.5	log2fc 7 vs. 7.5	log2fc 7.5 vs. 8	log2fc 7 vs. 9	log2fc 8 vs. 9
rs6874700	HMGB1P47	n.e.			HMGB1P47	-2.00	0.00	-2.00	activated	-3.00	suppressed
rs6874700	ISL1-DT	n.e.			ISL1-DT	-1.38	0.85	-0.53	-1.8	-1.61	0.00
rs10853087	LINC01974	n.e.			LINC01974			n.e.			
20:55165923	LINC01716	n.e.			LINC01716			n.e.			

Bold: differential expressed genes (log2fc <-1.5 or >1.5).
log2fc log2 fold change, vs. versus, Chr. chromosome, n.e. not expressed. Differential expression defined with log2fc <-1.5 or >1.5.

gene expression signatures of human bladder cancers¹⁹. *PAWR*, has been previously shown to be a key altered gene in human bladder cancer stem cells²⁰. *SYT1* has been reported as a possible oncogene in colon cancer²¹. The knockdown of *SYT1* markedly inhibits colon cancer cell proliferation, migration, and invasion, and induces cell apoptosis, indicating that *SYT1* may function as an oncogene in colon cancer²¹. *ISL1* has been associated with high-risk non-muscle-invasive bladder cancer in several studies^{22,23}. Here we found downregulation of *ISL1* in embryonic stages of mouse and human CBE urogenital tissues. Vice versa we found dysregulation of *ISL1* expression in three bladder cancers. Hence, dysregulation of *ISL1* expression in human embryonic and adult bladder tissues might contribute to the CBE and bladder malignancies vice versa.

To date, this is the largest genetic study on CBE. We have identified eight genome-wide significant risk loci. Our transcriptomic analysis of CBE-relevant mouse embryonic, human embryonic, and fetal urogenital tissues suggests candidate genes within these loci. Bladder cancer transcriptomic suggests these candidate genes play a possible role in the CBE-associated bladder cancer susceptibility. Identification of the different expressions to turn these developmental genes on later in life might ultimately lead to preventive strategies for bladder cancer per se.

Methods

Patients and recruitment. This study was approved by the institutional ethics committee of each participating center. All experimental protocols were approved by the institutional committee of the University of Bonn (Lfd.Nr.031/19). The study was conducted according to the Declaration of Helsinki principles. Written informed consent was obtained from all patients, guardians, and healthy controls. We included 420 newly recruited isolated CBE patients and 5,649 healthy controls of European origin. Details can be found in the Supplementary information (Supplementary Table 1). Details about the 208 CBE patients and 1,703 ethnically matched controls of our previous studies, included in the present meta-analysis, are described in [5,6], in summary, CBE patients were recruited under written informed consent by BEEC expert physicians.

Sample description. In addition to the two previously described samples GWAS1 and GWAS2⁶, five new samples of patients with bladder exstrophy and

representative controls were obtained from Central Europe, the United Kingdom, Italy, Spain, and Sweden. The number of cases and controls used in this study are shown in Supplementary Information (Supplementary Table 1).

Genotyping. All samples, cases, and controls, were genotyped on Illumina human genotyping arrays. In GWAS 1 (Reutter et al. 2014), cases and controls were genotyped in two batches. Due to the discontinuation of the genotyping arrays utilized for earlier batches, different arrays were used comprising Illumina's Human610-Quad (H610Q) and Human660W-Quad Bead Chips and the Illumina HumanOmni1-Quad-v1 Bead Chip. In GWAS 2⁶, all cases and controls were genotyped using the Illumina BeadChip HumanOmniExpress. The five novel GWAS case samples were newly genotyped simultaneously using the Illumina "Infinium Global Screening Array-24 v2.0". The five novels ethnically matched control samples were also genotyped using the Illumina "Infinium Global Screening Array-24 v2.0". However, the five novel control samples were not genotyped together with the five novel case samples but independently of each other.

Quality control of individuals. An individual was excluded if (i) the call rate was <97%; (ii) the rate of autosomal heterozygosity deviates more than six standard deviations from the mean; (iii) the rate of X-chromosomal heterozygous genotypes was >2% for a supposed male individual or <10% for a supposed female individual. PLINK version 1.9 and KING were used to detect pairs of closely related individuals within and between samples^{24,25}. From each pair of individuals with an estimated identity by descending probability >0.2 or kinship coefficient >0.0884, the individual with a higher rate of missing genotypes was discarded. Individuals being outliers in a multidimensional scaling analysis (MDS) were removed. The post-quality control sample sizes are presented in Supplementary Table 1.

Principal component analysis. Individuals with:

$$\left(\frac{c_1 - m_1}{s_1}\right)^2 + \left(\frac{c_2 - m_2}{s_2}\right)^2 \geq 81 \quad (1)$$

were considered to be outliers. c_1 and c_2 denote the first two MDS coordinates of the individual and m_1 , m_2 and s_1 and s_2 denote the mean and standard deviation, respectively, of the first two MDS coordinates in European HapMap individuals. For the five new samples (Central Europe, Italy, Spain, Sweden, and the UK), Supplementary Information (Supplementary Figs. 9–13) show the first two MDS coordinates for all genotyped individuals together with Asian and African HapMap individual. For the samples of GWAS1 and GWAS2, the MDS coordinates used in our previous studies are shown in Supplementary Information (Supplementary Figs. 14, 15).

Quality control of variants and imputation. Separately in each of the different ethnicity samples, SNPs were removed if (i) the minor allele frequency was <1% in

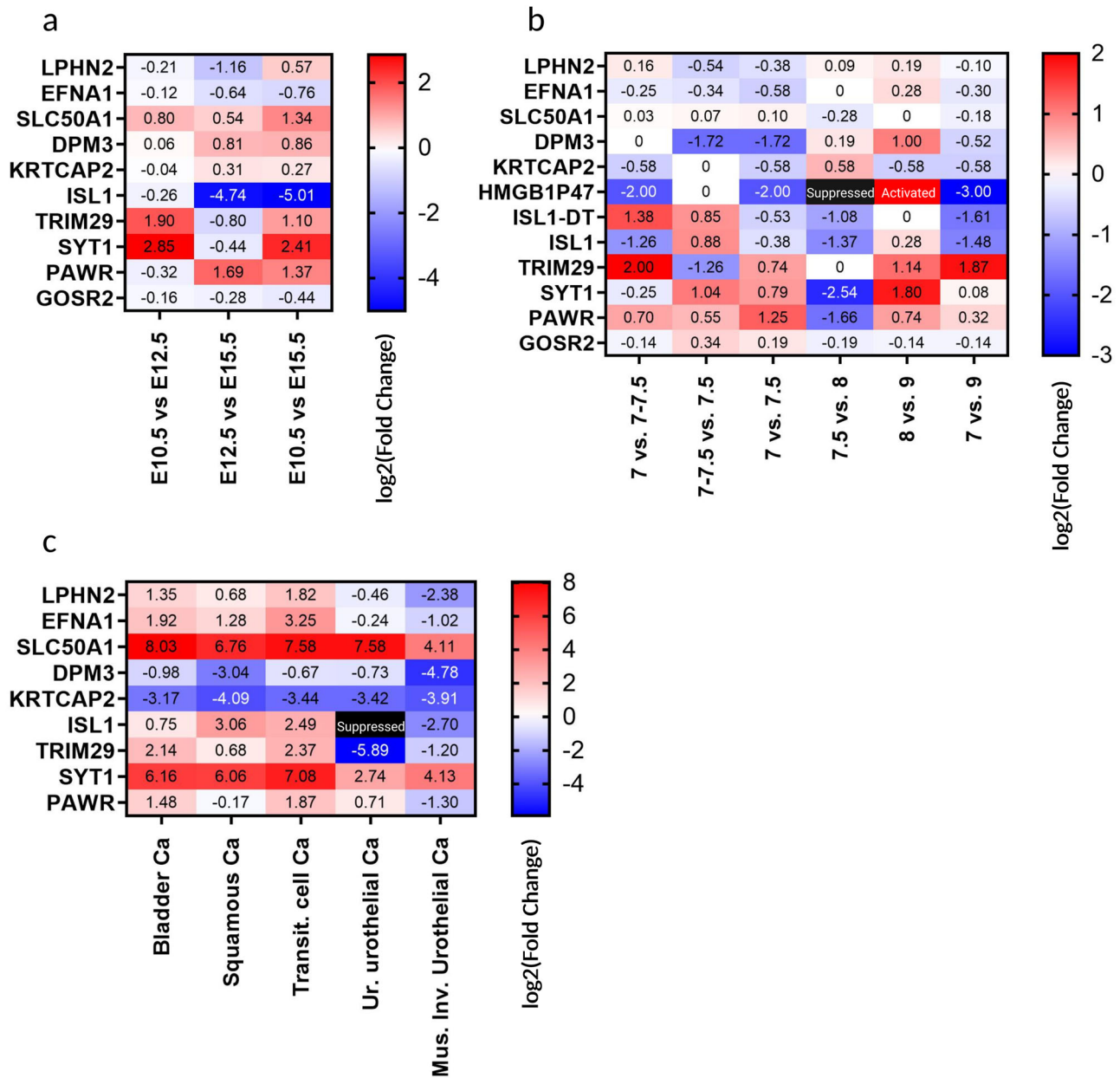


Fig. 2 Expression heatmaps of genes that reside in the LD blocks of the eight significant genetic markers. a Genes expression pattern in mouse embryonic bladder from embryonic day E10.5 to E12.5, E12.5 to E15.5, and E10.5 to E15.5. **b** Genes expression pattern in human embryonic and fetal bladder from week 7 to 7-7.5, 7-7.5 to 7.5, 7 to 7.5, 7.5 to 8, 8 to 9, and 7 to 9. **c** Genes expression pattern of 3-year-old control bladder tissue compared to Bladder carcinoma (Bladder Ca), Bladder squamous cell carcinoma (Squamous cell Ca), Bladder transitional cell carcinoma (Transit. cell Ca), Ureter urothelial carcinoma (Ur. Urothelial Ca), Muscle invasive urothelial cancer (Mus. Inv. Urothelial Ca). Legend: Suppressed = gene is silenced and no expression is detected. Activated = gene shows expression after a silenced state.

either cases or controls; (ii) the successful genotyping rate was >95% in either cases or controls; (ii) the *p* value for Hardy–Weinberg equilibrium was <10⁻⁴ in controls or <10⁻⁶ in cases. SNPs satisfying the quality filters were uploaded for imputation on the University of Michigan Imputation Server using the Haplotype Reference Consortium panel²⁶.

Statistical analysis for genome-wide association analysis. Association testing was performed by logistic regression using SNPTTEST version 2.5.2 for the allele dosage and adjusted for the sample-specific top five MDS coordinates²⁷. For each SNP, a meta-analysis with the fixed-effects inverse variance-weighting approach was conducted by including only those samples in which the info score was >0.4 and the mean dosage for the minor allele was >1% in cases and controls for the respective SNP. SNPs reaching a *p* value <5*10⁻⁸ in the meta-analysis are considered to be genome-wide significant. Q-Q and Manhattan plots for the meta-analysis were created by SAS²⁸. Regional association plots for genome-wide significant loci were generated with LocusZoom²⁹. To look for secondary signals of

association in loci of genome-wide significance, logistic regression using SNPTTEST conditioned on the most associated SNP in the locus was carried out.

Protein–protein interaction networks analysis. Putative candidate genes within identified risk loci were mapped to the STRING to acquire protein–protein interaction (PPI) networks (<https://string-db.org/>). The search tool integrates both known and predicted PPIs. Here it was used to predict functional interactions of proteins^{30,31}. Active interaction sources, including text mining, experiments, databases, and co-expression as well as species limited to “Homo sapiens” and an interaction score >0.4 were applied to construct the PPI networks. In the networks, the nodes correspond to the proteins and the edges represent the interactions. STRING was employed to seek potential interactions among putative candidate genes. Active interaction sources, including experimental repositories, computational prediction methods, and public text collections as well as species limited to “Homo sapiens” and a combined score >0.4, were applied.

Table 4 Average TPM of coding and non-coding genes in the LD blocks of the most significant GWAS markers calculated for each bladder cancer cell line.

Marker	Coding and non-coding genes	Control tissue	Bladder Ca	Transit. cell Ca	Squamous cell Ca	Ur. urothelial Ca	Mus. Inv. Urothelial Ca
rs1924557	LPHN2	6.87	17.47	24.25	11.00	5.00	1.32
rs4745	EFNA1	8.25	31.30	78.50	20.00	7.00	4.06
rs4745	SLC50A1	0.24	62.60	46.00	26.00	46.00	4.15
rs4745	DPM3	131.29	66.55	82.50	16.00	79.00	4.77
rs4745	KRTCAP2	170.89	18.95	15.75	10.00	16.00	11.37
rs6874700	ISL1	0.36	0.61	2.03	3.00	0.00	0.06
11:119964758	TRIM29	11.86	52.27	61.25	19.00	0.20	5.15
rs10862001	SYT1	0.06	4.30	8.13	4.00	0.40	1.05
rs10862001	PAWR	13.47	37.65	49.25	12.00	22.00	5.46
rs10853087	GOSR2	11.25	16.80	12.50	5.00	16.00	3.69
rs6874700	HMGB1P47	RNA-polyA-seq	0.00	0.00	0.00	0.00	RNA-polyA-seq
rs6874700	ISL1-DT	RNA-polyA-seq	0.11	0.20	0.5	0.00	RNA-polyA-seq
rs10853087	LINC01974	RNA-polyA-seq	0.04	0.00	0.00	0.00	RNA-polyA-seq
20:55165923	LINC01716	RNA-polyA-seq	0.01	0.00	0.00	0.00	RNA-polyA-seq

urothelial carcinoma tissues and control bladder tissue.

TPM for Non-coding genes in Control tissue and Muscular invasive urothelial cancer do not show reads due to polyA-sequencing. Legend: Bladder tissue of a 3-year-old bladder donor (control tissue); Bladder carcinoma (Bladder Ca); Bladder transitional cell carcinoma (Transit. cell Ca); Bladder squamous cell carcinoma (Squamous Ca); Ureter urothelial carcinoma (Urothelial Ca); Bladder urothelial carcinoma (Bl. urothelial Ca); Muscle invasive urothelial cancer (Mus. Inv. Urothelial Ca); RNA-polyA-seq data do not include miRNAs or lincRNAs.

Table 5 log₂-fold change of genes in the LD blocks of the most significant GWAS markers of bladder cancer cell types and muscle-invasive urothelial cancer over bladder control tissue.

Marker	Coding and non-coding genes	Control tissue vs. bladder Ca	Control tissue vs. transit. cell Ca	Control tissue vs. squamous cell Ca	Control tissue vs. Ur. urothelial Ca	Control tissue vs. Mus. Inv. urothelial Ca
rs1924557	LPHN2	1.35	1.82	0.68	0.46	− 2.38
rs4745	EFNA1	1.92	3.25	1.28	−0.24	−1.02
rs4745	SLC50A1	8.03	7.58	6.76	7.58	4.11
rs4745	DPM3	−0.98	−0.67	− 3.04	−0.73	− 4.78
rs4745	KRTCAP2	− 3.17	− 3.44	− 4.09	− 3.42	− 3.91
rs6874700	ISL1	0.75	2.49	3.06	suppressed	− 2.70
11:119964758	TRIM29	2.14	2.37	0.68	− 5.89	−1.20
rs10862001	SYT1	6.16	7.08	6.06	2.74	4.13
rs10862001	PAWR	1.48	1.87	−0.17	0.71	−1.30
rs10853087	GOSR2	0.54	0.12	−1.21	−0.47	− 1.65
rs6874700	HMGB1P47	RNA-polyA-seq	RNA-polyA-seq	RNA-polyA-seq	RNA-polyA-seq	RNA-polyA-seq
rs6874700	ISL1-DT	RNA-polyA-seq	RNA-polyA-seq	RNA-polyA-seq	RNA-polyA-seq	RNA-polyA-seq
rs10853087	LINC01974	RNA-polyA-seq	RNA-polyA-seq	RNA-polyA-seq	RNA-polyA-seq	RNA-polyA-seq
20:55165923	LINC01716	RNA-polyA-seq	RNA-polyA-seq	RNA-polyA-seq	RNA-polyA-seq	RNA-polyA-seq

Bold: differential expressed genes (log₂fc <−1.5 or >1.5)

Log₂ fold change for non-coding genes of different bladder cancers and Muscular Invasive Urothelial cancer over control tissue shows no value due to polyA-sequencing of control tissue. Differential Expression defined with log₂fc <−1.5 or >1.5 (marker in bold italic letters). Legend: Bladder tissue of a 3-year-old bladder donor (control tissue); Bladder carcinoma (Bladder Ca); Bladder transitional cell carcinoma (Transit. cell Ca); Bladder squamous cell carcinoma (Squamous Ca); Ureter urothelial carcinoma (Urothelial Ca); Bladder urothelial carcinoma (Bl. urothelial Ca); Muscle invasive urothelial cancer (Mus. Inv. Urothelial Ca); RNA-polyA-seq data does not include miRNAs or lincRNAs). log₂fc log₂ fold change; differential expression defined with log₂fc <−1.5 or >1.5 (marker in bold italic letters). vs. versus, Chr. chromosome.

Re-sequencing of EFNA1. Re-sequencing of all coding exons of *EFNA1* of transcript ENST00000368407.3 was performed in 580 CBE patients, all of which were included in the current GWAS. PCR conditions can be obtained upon request, primer sequences are shown in Supplementary information (Supplementary Table 2). Sequencing files for patient, parent, and control DNA were added to databases created using PreGap4 software, with control DNA processed as the reference sequence.

Genes prioritization. Lower p-value SNP of each associated region was imputed in LDproxy Tool (<https://ldlink.nci.nih.gov/?tab=ldproxy>) for European populations of CEU (Utah residents from north and west Europe); TSI Toscani in Italy; FIN Finnish in Finland; GBR British in England and Scotland; IBS Iberian population in Spain. Out of this, genes that reside in the linkage disequilibrium blocks defined from LD variants of r² above 0.8 to the top SNPs were taken into consideration for this study (Supplementary information, Supplementary Figs. 1–8). LD blocks coordinate regions imputed in hg19 are described in Supplementary Information (Supplementary Table 3).

No variants were significant LD associated with rs1924557 in chromosome 1 to determine an LD block region.

RNA isolation and mRNA library preparation of mouse embryonic urinary bladder and genital tissues. Animals were anesthetized with Isoflurane and sacrificed by cervical dislocation. Ethical consent is documented and approved by the local authorities of the Regierungspräsidium Darmstadt. Embryos from timed-pregnant females of the SWISS strain were harvested at embryonic days (E) E10.5, E12.5, and E15.5 (Supplementary information: Supplementary Fig. 18). The respective developmental Thiler stages were determined as 18 (TS18), TS21, and TS23. From E10.5 embryos, the urogenital ridge was dissected under an M205C stereo microscope (Leica Microsystems, Germany) surgically isolated, and transferred into QIAzol®. Embryos were pooled for each time point. For E10.5 stage biopsies from three embryos were pooled biopsies to prepare RNA, for E12.5 and E15.5 stages two embryos were pooled for RNA preparation. From E12.5 (primitive bladder) and E15.5 (bladder) embryos, the distinct structures of the developing and distinct visible bladder were surgically isolated (Supplementary information: Supplementary Fig. 18), combined, and transferred into QIAzol®.

Processing of total mouse embryonic RNA-sequencing data. About 50 million unique mapped reads per sample were obtained from each RNA-seq experiment. The reads were aligned using STAR aligner³². Read count was calculated with GenomicFeatures Bioconductor package. Calculation and normalization of “transcripts per kilobase million (TPM)” accounting for reads per kilobase (RPK) was performed as described elsewhere³³. The fold change was calculated by dividing the subsequent stage by the preceding one and the log₂ function was applied to the division as following: $\log_2(\text{FoldChange}) = \log_2(\text{subsequent embryonic stage/preceding embryonic stage})$. Differentially expressed genes were identified with values less than or equal to -1.5 or ≥ 1.5 , respectively. The same algorithm was applied for the calculation of TPM of already deposited human embryonic and fetal RNA-seq data at EMBL-EBI expression atlas (accession code: E-MTAB-6592).

The raw RNA-sequencing data of mouse embryonic urinary bladder are deposited at GEO with the accession id: [GSE190641](https://www.ncbi.nlm.nih.gov/geo/query/acc.cgi?acc=GSE190641).

Processing of bladder cancer RNA-sequencing data. Total RNA was purified using the QuantSeq library (Lexogen) with 500 ng RNA input. QuantSeq polyA RNA-tail libraries were sequenced (Single end 1 × 75 bp) on an Illumina HiSeq platform and generated data were further processed according to the GRCh38, TPM transformed, and further normalized. Sequencing, aligning and TPM calculation was performed by ImmunityBio™. Visualization of results in heatmaps was performed using graphpad PRISM 9.0.0.

RNA isolation and mRNA library preparation of human embryonic and fetal urinary bladder and genital tissues. Embryonic and fetal bladders and genital tissues were obtained by surgeons from terminated pregnancies after informed consent was obtained and with ethics approval. Pregnancies were terminated for social indications and the respective fetuses and embryos were healthy. The embryonic tissues comprised 7-week embryos, 7–7.5-week embryos, 7.5-week embryos, late 8-week embryos, and late 9-week embryos (Supplementary information: Supplementary Fig. 19). Samples comprised week 7 ($n = 2$), 7.5 ($n = 1$), 8 ($n = 3$), 9 ($n = 4$) for the bladder tissues and for the genital tissues from week 7 ($n = 3$), 8 ($n = 3$), 9 ($n = 3$), and 10 ($n = 4$). Gene expression data were extracted and analyzed after high throughput sequencing of paired-end mRNA libraries (Illumina). Data were deposited at EMBL-EBI expression atlas (accession code: E-MTAB-6592). Calculation of fold change of already deposited human embryonic RNA-seq data was carried out accordingly to our calculation of mouse embryonic data (see in Methods: Processing of total mouse embryonic RNA-sequencing data).

Processing of bladder cancer RNA-sequencing data. Cancer RNA-seq data were obtained from already deposited data at EMBL-EBI expression atlas (Cancer Cell Line Encyclopedia, experiment E-MTAB-2770). The deposited data does not include samples derived from CBE patients. Out of 1019 different cancer cell lines, the following cell line sample has been analyzed: 20 cell lines of bladder carcinoma, one cell line of bladder squamous cell carcinoma, four cell lines of bladder transitional cell carcinoma, one cell line of ureter urothelial carcinoma. TPM average was then calculated for each carcinoma cell type and data were compared with fold change to TPM of deposited mature urinary bladder polyA RNA-seq data (GEO accession: [GSM1067793](https://www.ncbi.nlm.nih.gov/geo/query/acc.cgi?acc=GSM1067793)). In addition, RNA-polyA-seq data available from 38 cases of the CCC-EMN bladder cancer cohort [12] were generated from FFPE tissue all classified with Muscular invasive urothelial carcinoma. Demographic data is found in Supplementary Data 1.

Statistics and reproducibility. Quality control of individuals, principal component analysis, Quality control of variants and imputation, Statistical analysis for GWAS, and Genes prioritization is meticulously described in the methods above.

Average of TPM was calculated in R from biological replicates. Log₂FC of human and mouse bladder was calculated as following: $\log_2(\text{AVERAGE_TPM}_{\text{next_stage}}/\text{AVERAGE_TPM}_{\text{previous_stage}})$. Log₂FC of cancer cells was calculated as following: $\log_2(\text{AVERAGE_TPM}_{\text{cancer_line}}/\text{AVERAGE_TPM}_{\text{control_bladder_tissue}})$. Sample size of mouse consists in $n = 3$ for embryo bladder at stage E10.5, and $n = 2$ for E12.5 and E15.5. Human fetal bladder samples comprised week 7 ($n = 2$), 7.5 ($n = 1$), 8 ($n = 3$), 9 ($n = 4$). Human cancer cells lines comprised $n = 20$ of bladder carcinoma cell, $n = 1$ of bladder squamous cell carcinoma cell line, $n = 4$ of bladder transitional cell carcinoma cell lines, $n = 1$ of ureter urothelial carcinoma cell line, $n = 38$ of muscular invasive urothelial carcinoma. Replicates are defined as a minimum of three technical replicates per sample size.

Reporting summary. Further information on research design is available in the Nature Research Reporting Summary linked to this article.

Data availability

GWAS generated and analyzed data during this study are included in this article and its supplementary information files. GWAS data are deposited at NHGRI-EBI GWAS Catalog with accession ID: [GCST90132313](https://www.ebi.ac.uk/gwas/studies/GCST90132313). EFNA1 DNA sequencing data are deposited in GeneBank (BankIt) with the following accession numbers: [OP312051](https://www.ncbi.nlm.nih.gov/nuccore/OP312051); [OP312052](https://www.ncbi.nlm.nih.gov/nuccore/OP312052); [OP312053](https://www.ncbi.nlm.nih.gov/nuccore/OP312053); [OP312054](https://www.ncbi.nlm.nih.gov/nuccore/OP312054); [OP312055](https://www.ncbi.nlm.nih.gov/nuccore/OP312055); [OP312056](https://www.ncbi.nlm.nih.gov/nuccore/OP312056); [OP312057](https://www.ncbi.nlm.nih.gov/nuccore/OP312057); [OP312058](https://www.ncbi.nlm.nih.gov/nuccore/OP312058); [OP312059](https://www.ncbi.nlm.nih.gov/nuccore/OP312059);

[OP312060](https://www.ncbi.nlm.nih.gov/nuccore/OP312060); [OP312061](https://www.ncbi.nlm.nih.gov/nuccore/OP312061); [OP312062](https://www.ncbi.nlm.nih.gov/nuccore/OP312062); [OP312063](https://www.ncbi.nlm.nih.gov/nuccore/OP312063). The raw RNA-sequencing data of the 38 Muscular Invasive Urothelial carcinomas are deposited at NCBI in Sequence Read Archive (SRA) with the following BioProject accession: [PRJNA882449](https://www.ncbi.nlm.nih.gov/bioproject/PRJNA882449). The raw RNA-sequencing data of mouse embryonic urinary bladder are deposited at GEO with the accession id: [GSE190641](https://www.ncbi.nlm.nih.gov/geo/query/acc.cgi?acc=GSE190641). The raw RNA-sequencing data of human embryonic and fetal urinary bladder and genital tissue are deposited at EMBL-EBI expression atlas with the following accession id: [E-MTAB-6592](https://www.ebi.ac.uk/ena/arrayexpress/experiments/E-MTAB-6592). The raw RNA-sequencing data of cancer cell lines are obtained from EMBL-EBI expression atlas with the following accession id: [E-MTAB-2770](https://www.ebi.ac.uk/ena/arrayexpress/experiments/E-MTAB-2770). PolyA RNA-sequencing of the mature urinary bladder is obtained from GEO with the following accession id: [GSM1067793](https://www.ncbi.nlm.nih.gov/geo/query/acc.cgi?acc=GSM1067793).

Received: 23 February 2022; Accepted: 11 October 2022;

Published online: 09 November 2022

References

- Ebert, A.-K., Reutter, H., Ludwig, M. & Rösch, W. H. The exstrophy-epispadias complex. *Orphanet J. Rare Dis.* **4**, 23 (2009).
- Dahm, P. & Gschwend, J. E. Malignant non-urothelial neoplasms of the urinary bladder: a review. *Eur. Urol.* **44**, 672–681 (2003).
- Williamson, S. R., Lopez-Beltran, A., Montironi, R. & Cheng, L. Glandular lesions of the urinary bladder: clinical significance and differential diagnosis. *Histopathology* **58**, 811–834 (2011).
- Ebert, A. K., Zwink, N., Reutter, H. M. & Jenetzky, E. A prevalence estimation of exstrophy and epispadias in Germany from Public Health Insurance Data. *Front. Pediatr.* **9**, 648414 (2021).
- Reutter, H. et al. Genome-wide association study and mouse expression data identify a highly conserved 32 kb intergenic region between WNT3 and WNT9b as possible susceptibility locus for isolated classic exstrophy of the bladder. *Hum. Mol. Genet.* **23**, 5536–5544 (2014).
- Draaken, M. et al. Genome-wide association study and meta-analysis identify ISL1 as genome-wide significant susceptibility gene for bladder exstrophy. *PLoS Genet.* **11**, 1005024 (2015).
- Rieke, J. M. et al. SLC20A1 is involved in urinary tract and urorectal development. *Front. Cell Dev. Biol.* **8**, 567 (2020).
- Itou, J. et al. Islet1 regulates establishment of the posterior hindlimb field upstream of the Hand2-Shh morphoregulatory gene network in mouse embryos. *Development* **139**, 1620–1629 (2012).
- Bult, C., Blake, J., Smith, C., Kadin, J. & Richardson, J. Mouse Genome Database (MGD) 2019. *Nucleic Acids Res.* **47**, D801–D806 (2019).
- Masden, T. B., Taela, A., Rocha, M., da Moores, D. C. & Radulescu, A. Isolated thoracoschisis with rib agenesis and liver herniation: a case report. *Am. J. Case Rep.* **20**, 1915–1919 (2019).
- Lek, M. et al. Exome Aggregation Consortium. Analysis of protein-coding genetic variation in 60,706 humans. *Nature* **536**, 285–291 (2016).
- Zhang, S. et al. Transcriptome profiling of a multiple recurrent muscle-invasive urothelial carcinoma of the bladder by deep sequencing. *PLoS One* **9**, 91466 (2014).
- Hao, Y. & Li, G. Role of EFNA1 in tumorigenesis and prospects for cancer therapy. *Biomed. Pharmacother.* **130**, 110567 (2020).
- Toma, M. I. et al. Lack of ephrin receptor A1 is a favorable independent prognostic factor in clear cell renal cell carcinoma. *PLoS One* **9**, 102262 (2014).
- Warrington, N. M. et al. Genome-wide association study identifies nine novel loci for 2D:4D finger ratio, a putative retrospective biomarker of testosterone exposure in utero. *Hum. Mol. Genet.* **27**, 2025–2038 (2018).
- Eeles, R. A. et al. Identification of 23 new prostate cancer susceptibility loci using the iCOGS custom genotyping array. *Nat. Genet.* **45**, 385–391 (2013).
- Popiołek, A. et al. Prostate-specific antigen and testosterone levels as biochemical indicators of cognitive function in prostate cancer survivors and the role of diabetes. *J. Clin. Med.* **10**, 5307 (2021).
- Liu, J., Welm, B., Boucher, K. M., Ebbert, M. T. W. & Bernard, P. S. TRIM29 functions as a tumor suppressor in nontumorigenic breast cells and invasive ER+ breast cancer. *Am. J. Pathol.* **180**, 839–847 (2012).
- Palmbo, P. L. et al. ATDC/TRIM29 drives invasive bladder cancer formation through miRNA-mediated and epigenetic mechanisms. *Cancer Res.* **75**, 5155–5166 (2015).
- Yang, Z. et al. Single-cell sequencing reveals variants in ARID1A, GPRC5A and MLL2 driving self-renewal of human bladder cancer stem cells. *Eur. Urol.* **71**, 8–12 (2017).
- Lu, H., Hao, L., Yang, H., Chen, J. & Liu, J. miRNA-34a suppresses colon carcinoma proliferation and induces cell apoptosis by targeting SYT1. *Int. J. Clin. Exp. Pathol.* **12**, 2887–2897 (2019).

22. Gurung, P. et al. Prognostic DNA methylation biomarkers in high-risk non-muscle-invasive bladder cancer: a systematic review to identify loci for prospective validation. *Eur. Urol. Focus* **6**, 683–697 (2020).
23. Kitchen, M. O. et al. Methylation of HOXA9 and ISL1 predicts patient outcome in high-grade non-invasive bladder cancer. *PLoS One* **10**, 0137003 (2015).
24. Purcell, S. et al. PLINK: a tool set for whole-genome association and population-based linkage analyses. *Am. J. Hum. Genet.* **81**, 559–575 (2007).
25. Manichaikul, A., Palmer, A. A., Sen, S. & Broman, K. W. Significance thresholds for quantitative trait locus mapping under selective genotyping. *Genetics* **177**, 1963–1966 (2007).
26. Das, S. et al. Next-generation genotype imputation service and methods. *Nat. Genet.* **48**, 1284–1287 (2016).
27. Marchini, J., Howie, B., Myers, S., McVean, G. & Donnelly, P. A new multipoint method for genome-wide association studies via imputation of genotypes: Supplementary Methods Imputation of missing genotypes Imputation of completely missing SNPs. *Nat. Genet.* **39**, 906–913 (2007).
28. SAS Institute Inc. 2013. SAS 9.4 Language Reference. Cary, NC: SAS Institute.
29. Pruim, R. J. et al. LocusZoom: regional visualization of genome-wide association scan results. *Bioinformatics* **26**, 2336–2337 (2011).
30. Szklarczyk, D. et al. STRING v10: protein-protein interaction networks integrated over the tree of life. *Nucleic Acids Res.* **43**, 447–452 (2015).
31. Wullweber, A. et al. Bladder tumor subtype commitment occurs in carcinoma in situ driven by key signaling pathways including ECM Remodeling. *Cancer Res.* **81**, 1552–1566 (2021).
32. Dobin, A. et al. STAR: ultrafast universal RNA-seq aligner. *Bioinformatics* **29**, 15–21 (2013).
33. Li, B., Ruotti, V., Stewart, R. M., Thomson, J. A. & Dewey, C. N. RNA-Seq gene expression estimation with read mapping uncertainty. *Bioinformatics* **26**, 493–500 (2009).

Acknowledgements

We acknowledge the following institutions and organizations for founding and/or contributing to the project: BONFOR; Instituto de Salud Carlos III; Medical Research Council; Horizon 2020 Marie Skłodowska-Curie Actions Initial Training Network; RENALTRACT; Alzheimer Research UK; Stroke Foundation/British Heart Foundation. We acknowledge financial support by Deutsche Forschungsgemeinschaft and Friedrich-Alexander-Universität Erlangen-Nürnberg within the funding programme “Open Access Publication Funding”.

Author contributions

E.M., B.O., P.G., M.K., W.N., G.B., A.N., A.S.W., and H.R. conceptualized and supervised the research. E.M., M.K., G.C.D., and M.E. C.M., were engaged in biostatistics and bioinformatics analysis. E.M., P.G., M.E. B.O., P.G., H.R., A.S.W., A.C.H., and G.B. designed and performed most experiments. W.R., A.-K.E., R.S., A.B., M.D.G., A.T., F.M.T., J.L.H., P.E., J.M.O., J.A.R., C.V., I.C.H., H.H., D.J.W., J.S., J.G., A.-S.G., B.C.B., S.A., E.Á., E.R., M.L., G.H., E.G., A.B., D.K., R.M.C., N.Y., M.O., J.O., B.H., M.P., C.N.,

K.H., M.S., F.-M.S., E.S., T.M.B., I.A.L.M.v.R., W.F.J.F., C.L.M.M., M.L., J.N., B.U., C.F., D.P.G., M.M.Y.C., K.U.L., M.M.N., S.H., N.Z., E.J. were responsible for patient recruitment and biospecimen and clinical data collection. E.M., G.B., M.K., A.S.W., P.G., and H.R. drafted the manuscript. E.M. designed the graphic illustrations. All authors reviewed and edited the manuscript. All author(s) read and approved the final manuscript.

Funding

Open Access funding enabled and organized by Projekt DEAL.

Competing interests

The authors declare no competing interests.

Additional information

Supplementary information The online version contains supplementary material available at <https://doi.org/10.1038/s42003-022-04092-3>.

Correspondence and requests for materials should be addressed to Enrico Mingardo or Heiko Reutter.

Peer review information *Communications Biology* thanks Jack Weaver and the other, anonymous, reviewer(s) for their contribution to the peer review of this work. Primary Handling Editors: Chiea Chuen Khor and George Inglis.

Reprints and permission information is available at <http://www.nature.com/reprints>

Publisher's note Springer Nature remains neutral with regard to jurisdictional claims in published maps and institutional affiliations.



Open Access This article is licensed under a Creative Commons Attribution 4.0 International License, which permits use, sharing, adaptation, distribution and reproduction in any medium or format, as long as you give appropriate credit to the original author(s) and the source, provide a link to the Creative Commons license, and indicate if changes were made. The images or other third party material in this article are included in the article's Creative Commons license, unless indicated otherwise in a credit line to the material. If material is not included in the article's Creative Commons license and your intended use is not permitted by statutory regulation or exceeds the permitted use, you will need to obtain permission directly from the copyright holder. To view a copy of this license, visit <http://creativecommons.org/licenses/by/4.0/>.

© The Author(s) 2022

¹Institute for Anatomy and Cell Biology, University Hospital Bonn, University of Bonn, Bonn, Germany. ²Institute for Neuroanatomy, University Hospital Bonn, University of Bonn, Bonn, Germany. ³Institute of Human Genetics, School of Medicine & University Hospital Bonn, University of Bonn, Bonn, Germany. ⁴Centre for Genomic Medicine, University of Manchester, Manchester, UK. ⁵Institute of Cardiovascular Regeneration, Centre for Molecular Medicine, Goethe University, Frankfurt am Main, Germany. ⁶Georg-Speyer-Haus, Frankfurt am Main, Germany. ⁷Department of Women's and Children's Health and Center for Molecular Medicine, Karolinska Institutet, Stockholm, Sweden. ⁸Pediatric Surgery, Astrid Lindgren Children Hospital, Karolinska University Hospital, Stockholm, Sweden. ⁹Division of Cell Matrix Biology and Regenerative Medicine, Faculty of Biology Medicine and Health, School of Biological Sciences, University of Manchester, Manchester, UK. ¹⁰Royal Manchester Children's Hospital, Manchester University NHS Foundation Trust, Manchester Academic Health Science Centre, Manchester, UK. ¹¹Institute of Pathology, University Hospital Erlangen, Friedrich-Alexander-University Erlangen-Nürnberg, Erlangen, Germany. ¹²Comprehensive Cancer Center Erlangen-EMN (CCC ER-EMN), Erlangen, Germany. ¹³BRIDGE-Consortium Germany e.V., Mannheim, Germany. ¹⁴Department of Pediatrics and Adolescent Medicine, University Hospital Erlangen, Erlangen, Germany. ¹⁵Department of Pediatric Urology, Clinic St. Hedwig, University Medical Center of Regensburg, Regensburg, Germany. ¹⁶Department of Urology and Pediatric Urology, University Hospital of Ulm, Ulm, Germany. ¹⁷Center for Pediatric, Adolescent and Reconstructive Urology, University Medical Center Mannheim, Heidelberg University, Mannheim, Germany. ¹⁸Department of Medical Sciences and Medical Genetics Unit, Città della Salute e della Scienza University Hospital, University of Torino, Torino, Italy. ¹⁹Institute for Maternal and Child Health, IRCCS Burlo Garofalo, Trieste, Italy. ²⁰Translational Pediatrics and Infectious Diseases, Hospital Clínico Universitario de Santiago, Santiago de Compostela, Spain. ²¹Department of Internal Medicine, Hospital U M Valdecilla, University of Cantabria, IDIVAL, Santander, Spain. ²²Department of Urology and Urosurgery, Medical Faculty Mannheim, University of Heidelberg, Mannheim, Germany. ²³Institute of Genomic Statistics and Bioinformatics, University of Bonn, Bonn, Germany. ²⁴Department of Internal Medicine. Hospital U M Valdecilla, University of Cantabria, IDIVAL, Santander, Spain. ²⁵Stroke Research Centre, University College London, Institute of Neurology, London, UK. ²⁶Neurogenetics Laboratory, The National Hospital of Neurology and Neurosurgery, London, UK. ²⁷Department of Neurosurgery, Klinikum rechts der Isar, Technical University Munich, Munich, Germany. ²⁸Neurogenetics Laboratory, The National Hospital of Neurology and Neurosurgery, London, UK. ²⁹Stroke Research Center, Department of Brain Repair and Rehabilitation, UCL

Institute of Neurology and The National Hospital for Neurology and Neurosurgery, London, UK. ³⁰Institute for Human Genetics, University of Marburg, Marburg, Germany. ³¹Department of Women's and Children's Health and Center for Molecular Medicine, Bioclinicum, Karolinska Institutet, Stockholm, Sweden. ³²Department of Urology, Danderyds Hospital, Danderyd, Sweden. ³³Division of Neurogeriatrics, Department of Neurobiology, Care Sciences and Society, Karolinska Institutet, Stockholm, Sweden. ³⁴R&D Unit, Stockholms Sjukhem, Stockholm, Sweden. ³⁵ME Gynecology and Reproduction Medicine, Karolinska University Hospital, and Dept of Clintec, Karolinska Institutet, Stockholm, Sweden. ³⁶Department of Clinical Chemistry and Clinical Pharmacology, University of Bonn, Bonn, Germany. ³⁷Department of Pediatric Surgery, Queen Silvia Children's Hospital, Gothenburg, Sweden. ³⁸Department of Molecular Medicine, University of Pavia, Pavia, Italy. ³⁹Laboratory of Molecular Medicine and Cytogenetics, IRCCS Mondino Foundation, Pavia, Italy. ⁴⁰Pediatric Urology Unit, Fondazione IRCCS Ca' Granda Ospedale Maggiore Policlinico, Milan, Italy. ⁴¹Paediatric Urology, Royal Manchester Children's Hospital, Central Manchester University Hospitals NHS Foundation Trust, Manchester, UK. ⁴²Department for Pediatric Urology, Ordensklinikum Linz, Hospital of the Sisters of Charity, Linz, Austria. ⁴³Division of Pediatric Urology, Department of Urology, University of Erlangen-Nürnberg, Erlangen, Germany. ⁴⁴Department of Pediatric Surgery and Urology, Klinik Hallerwiese-Cnopfsche Kinderklinik, Nürnberg, Germany. ⁴⁵Department of Urology and Pediatric Urology, University Hospital Erlangen, Friedrich-Alexander-University Erlangen-Nürnberg, Erlangen, Germany. ⁴⁶Clinic for Paediatric Surgery and Paediatric Urology, Klinikum Bremen-Mitte, Bremen, Germany. ⁴⁷Department of Pediatric Surgery and Urology, University Hospital Cologne, Cologne, Germany. ⁴⁸Department of Pediatric Surgery, University of Leipzig, Leipzig, Germany. ⁴⁹Department for Health Evidence, Radboud Institute for Health Sciences, Radboud University Medical Center, Nijmegen, Netherlands. ⁵⁰Department of Urology, Pediatric Urology Center, Radboud University Nijmegen Medical Center, Nijmegen, The Netherlands. ⁵¹Department of Genetics, Radboud University Nijmegen Medical Center, Nijmegen, The Netherlands. ⁵²Center of Pediatric Surgery Hannover, Hannover Medical School, Hannover, Germany. ⁵³Department of Renal Medicine, University College London, London, UK. ⁵⁴Department of Genomics, Life & Brain Center, University of Bonn, Bonn, Germany. ⁵⁵Department of Child and Adolescent Psychiatry, University Medical Center of the Johannes Gutenberg University Mainz, Mainz, Germany. ⁵⁶Faculty of Health, School of Medicine, University of Witten/Herdecke, Witten, Germany. ⁵⁷Institute of Medical Biometry, Informatics, and Epidemiology, University of Bonn, Bonn, Germany. ⁵⁸Division of Neonatology and Pediatric Intensive Care Medicine, Department of Pediatric and Adolescent Medicine, Friedrich-Alexander-University Erlangen-Nürnberg, Erlangen, Germany. ⁵⁹These authors contributed equally: Enrico Mingardo, Glenda Beaman, Philip Grote, Michael Knapp, Heiko Reutter. ✉email: enming@uni-bonn.de; Heiko.Reutter@uk-erlangen.de